TES STUDY OF LOW-ALEBDO INTRACRATER DEPOSITS WITHIN AMAZONIS PLANITIA, MARS.

K. R. Stockstill[1,2], F. S. Anderson[1,2] and V. E. Hamilton[1], [1]Hawai'i Institute of Geophysics and Planetology, University of Hawai'I, 1680 East-West Road, POST 602B, Honolulu, HI 96822, [2]University of Hawai'i NASA Astrobiology Institute.

Introduction: More than 25% of Martian craters within 50° of the equator contain localized deposits of materials that are coarser and darker than the surrounding materials [1,2,3]. Schneider and Hamilton [4] studied a low-albedo, intracrater deposit within an Amazonis Planitia crater (here "crater 17", located at 17.92°N, 190.26°E) using visible, thermal and spectral data. Their study found that the mineralogy of the low-albedo deposits are dominated by mafic mineralogy (pyroxene and olivine) and that the derived bulk chemistry indicates an ultramafic lithology with the lowest silica contents currently found on Mars [4]. Another investigation of 23 intracrater deposits in the Amazonis Planitia region indicates both spectral and compositional variations among these deposits using THEMIS data [5]. That study divided the craters into two groups based on the spectral shape of their THEMIS apparent emissivity ratio spectrum, with a pyroxene-rich group and a basaltic group [5]. In addition, [6] studied the low-albedo deposits within 13 craters of the Amazonis Planitia region using TES data, which also divided the features into two distinct compositional groups. Group #1 was mafic rich (>40% mafic minerals) with low (<10%) feldspar abundance while group #2 was less mafic rich (30-40% mafic minerals) with higher (>20%) feldspar abundance [6]. This study builds upon these findings by refining the spectral library used to derive the mineralogy of the low-albedo deposits for 11 craters within the Amazonis Planitia Region (Fig. 1).

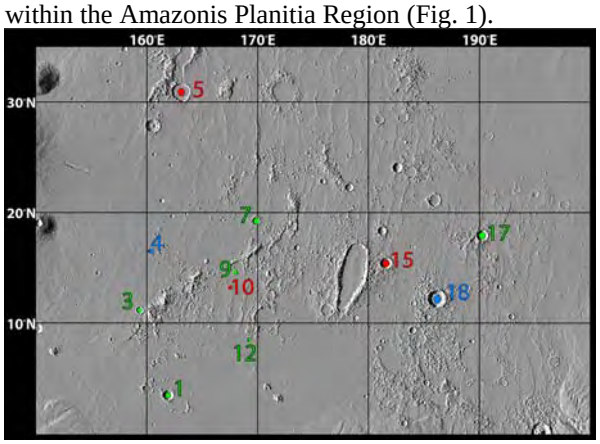

Figure 1: *Eleven craters in Amazonis Planitia containing low-albedo deposits explored in this study. Craters labeled in red have a foidite composition, craters labeled in green have a picrobasalt composition and craters labeled in blue are basaltic.*

Data: The Mars Global Surveyor (MGS) Thermal Emission Spectrometer (TES) acquired infrared radiance and emissivity data with a spatial resolution of 3 x 6 km, a spectral sampling of 5-cm^{-1} or 10-cm^{-1} and ranging from ~6-50 μm. TES also acquired broadband visible (0.3 – 2.7 μm) data as well as data from thermal (5-100 μm) bolometers providing albedo and thermophysical information of the Martian surface.

Methods: We examined TES spectra that overlap the low-albedo deposits of Amazonis Planitia craters; data were selected to have low albedo (<0.19), high brightness temperature (>255 K), low atmospheric dust (<0.20) and water opacity (<0.10) and overall data quality (e.g., avoiding data with "ringing"). Of the 23 Amazonis Planitia craters examined, we found satisfactory TES spectra for eleven of the low-albedo intracrater features (Fig. 1). TES spectra were extracted for the low-albedo dunes as well as the adjacent bright (dusty) crater floor for comparison; the latter will not be discussed here.

The average TES surface spectrum for each low-albedo deposit and bright crater floor were derived via linear deconvolution. Our end member set is a refinement of the set used by [4] and includes spectra of eight atmospheric end members, a surface dust end member, and mineral end members including feldspars, clinopyroxenes, orthopyroxenes, olivines, oxides, clays and glass end members. The major differences in our end member set are: 1) the olivine end members were contrast adjusted after [7] and 2) carbonate end members were excluded. In the process of examining prior deconvolution results, we determined that carbonates were being included to mimic the short wavelength contrast reduction of olivines observed by [7], not due to the presence of a carbonate absorption in the spectra.

Finally, we used the mineral abundances derived from linear deconvolution to calculate a bulk composition for each low-albedo deposit, similar to the method described by [8]. We then used these bulk compositions to assign the deposits to lithologic classes.

Results: For each of the 11 intracrater low-albedo deposit, we extracted 2 to 13 TES spectra from 1 to 3 orbits (Table 1). As with the findings of [4,6], our deconvolution results reflect a lithology that is rich in mafic minerals (olivine and pyroxene) and the pyroxene component is dominated by clinopyroxene (Table 1). In fact, our model of crater 17 [4] is the only

model that includes any orthopyroxene. In general, we see an increase in olivine abundance and decreases in pyroxene and feldspar abundances included in the models relative to [6]. Regardless, most TES surface emissivity spectra from this study strongly resemble the surface spectrum for crater 17 (Fig. 2). To variable degrees, the spectra display an absorption centered at ~900 cm^{-1} that matches well to olivine lab spectra; this may reflect variation in the olivine abundance within the deposits. Indeed, three spectra with the strongest olivine absorptions (3, 10, 12; Fig. 2) contain among the highest olivine abundances (Table 1).

When we converted our derived mineralogies to bulk chemical compositions, the low-albedo deposits are classified as ultramafic to mafic lithologies (38-47% SiO_2), as shown in Figure 3. Three craters (5, 10, 15) have lower derived SiO_2 abundances than the previously-studied crater 17 (Fig. 3) and plot within the foidite field. Five craters (1, 3, 7, 9, 12) plot with crater 17 in the picrobasalt field. Two remaining craters (4, 18) plot within the basaltic field.

Future work: We are presently working on relating the compositional variation to the craters' physiographic information and placing them in context of the regional geology.

References: [1] Arvidson, R.E. (1974) *Icarus, 21,* 12–27. [2] Sagan, C. *et al.* (1973) *JGR, 78,* 4,163–4,196. [3] Christensen, P.R. (1983) *Icarus, 56,* 496-518. [4] Schneider and Hamilton (2005) *JGR, 111,*, doi:10.1029/2005JE002611. [5] Schneider, R.D. *et al.* (2004) *LPSC XXXV*, #1470. [6] Schneider and Hamilton (2006) *LPSC XXXVII*, #1929. [7] Koeppen and Hamilton (2007) *JGR*, submitted. [8] Wyatt, M. *et al.* (2001) *JGR, 106,* 14,711-14,732.

Crater no.	Min. TES albedo	# spectra	Feldspars	Cpx	Opx	Olivine	Oxides	Clays	Glass	Sum
1	0.14	9	25	10	0	40	10	0	20	105
3	0.12	10	20	5	0	40	10	0	20	95
4	0.13	7	30	10	0	30	10	5	15	100
5	0.13	3	10	30	0	35	15	0	10	100
7	0.14	11	25	30	0	20	5	15	5	100
9	0.14	5	25	0	0	40	20	0	15	100
10	0.16	4	20	0	0	55	10	0	15	100
12	0.15	5	15	0	0	50	5	20	5	95
15	0.17	2	30	20	0	30	20	5	0	105
17	0.15	6	20	20	5	35	10	5	5	100
18	0.13	13	25	0	0	30	15	15	20	105

Table 1: *Deconvolution results normalized to remove atmosphere & surface dust, rounded to nearest 5%.*

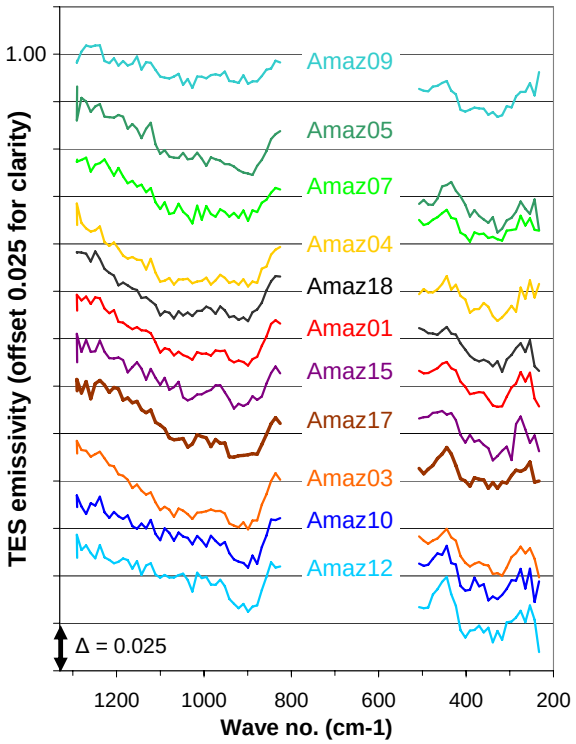

Figure 2: *TES surface spectra of low-albedo deposits in Amazonis Planitia craters. The crater 17 spectrum is shown in brown.*

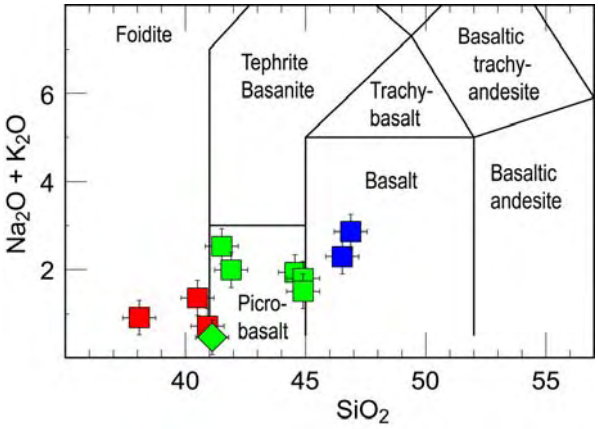

Figure 3: *Derived bulk chemistry for low-albedo deposits within Amazonis Planitia craters plotted on a part of the Total Alkali-Silica (TAS) diagram. Crater 17, previously studied by [4], is distinguished from other craters with a green diamond (41.1% SiO_2, 0.5% Na_2O+K_2O). Red symbols plot within foidite field, green symbols plot within the picrobasalt field and blue symbols plot within the basalt field. Error bars on symbols are standard deviations calculated by [8].*